Available online at www.sciencedirect.com

SciVerse ScienceDirect

Ceramics International 39 (2013) 2605–2610

CERAMICS INTERNATIONAL

www.elsevier.com/locate/ceramint

Synthesis of SiC/SiO_2 core–shell powder by rotary chemical vapor deposition and its consolidation by spark plasma sintering

Zhenhua He[a,b], Rong Tu[b,*], Hirokazu Katsui[a], Takashi Goto[a]

[a]*Institute for Materials Research, Tohoku University, Katahira 2-1-1, Aoba-ku, Sendai 980-8577, Japan*
[b]*Wuhan University of Technology, Wuhan 430070, PR China*

Received 8 August 2012; received in revised form 6 September 2012; accepted 7 September 2012
Available online 15 September 2012

Abstract

SiC (core) and SiO_2 (shell) powders were synthesized via rotary chemical vapor deposition (RCVD). The SiC particles (3C, <1 μm in diameter) were coated with a layer of SiO_2 (10–15 nm in thickness). Using spark plasma sintering, the SiC/SiO_2 nanopowders were then synthesized into SiC/SiO_2 composite bodies. Although a phase transformation from 3C to 6H was observed at above 2123 K in the sintered monolithic SiC bodies, sintered SiC/SiO_2 bodies did not display such phase transformation. In addition, SiC/SiO_2 bodies did not exhibited grain growth until the sintering temperature reached 2223 K. The density and Vickers hardness of the sintered SiC/SiO_2 bodies increased with increasing sintering temperature. The highest density and hardness of SiC/SiO_2 composite bodies were 98.1% and 24.4 GPa at 2223 K, respectively, which were higher than the corresponding values of 90% and 14 GPa for monolithic SiC bodies.

Keywords: Rotary chemical vapor deposition (RCVD); SiO_2 nano-layer; Silicon carbide (SiC); Spark plasma sintering (SPS)

1. Introduction

Silicon carbide (SiC) has been widely used to manufacture high-temperature materials because of its high oxidation resistance, high hardness and high thermal-shock resistance [1]. Monolithic SiC is hard to densify by conventional sintering techniques because of its highly covalent nature and the low self-diffusion of Si and C [2]. Therefore, high sintering temperature and the addition of sintering aids are normally required to enhance the densification process for SiC. During this densification process, the sintering additives form a second phase at grain boundaries. This second phase usually causes the mechanical and physical properties of the material to deteriorate, particularly at higher temperatures [3]. It has been shown that a SiC body can be fabricated by pressureless sintering with the aid of boron and carbon, and densified to more than 95% of the relative density at temperatures higher than 2323 K [4]. However, the low fracture toughness of such bodies limits their use in many potential structural applications [5].

Spark plasma sintering (SPS) is capable of fabricating dense bodies at relatively low temperatures in a short amount of time [6]. Zhou et al. densified SiC powder (with 30 nm diameter particles) doped with an Al_4C_3–B_4C additive to 99% of the relative density at 1873 K [7]. Ohyanagi et al. demonstrated the densification of a SiC powder (with 5–10 nm diameter particles) by high-energy mechanical milling to 98% of the relative density at 1973 K without using any additives [8].

Ye et al. densified a SiC powder with a 20 mass% SiO_2 additive to 94.2% of the relative density at 2133 K in a high-pressure CO gas atmosphere by liquid-phase sintering [9]. It is known that SiO_2 can be easily sintered [10], and can thus be used as a possible sintering additive to promote the densification of SiC. However, SiO_2 might degrade the mechanical properties of the SiC because of its low hardness and brittleness [11]. To use SiO_2 as a sintering aid for SiC such that its mechanical properties at least do not degrade, SiO_2 should be uniformly dispersed on the nanometer scale within the body. However, to the best of our knowledge, no such study has ever been performed. By

*Corresponding author at: State Key Lab of Advanced Technology for Materials Synthesis and Processing, Wuhan University of Technology, 122 Luoshi Road, Wuhan 430070, PR China.
Tel.: +86 151 72418915; fax: +86 27 87879468.
E-mail address: turong@whut.edu.cn (R. Tu).

0272-8842/$ - see front matter © 2012 Elsevier Ltd and Techna Group S.r.l. All rights reserved.
http://dx.doi.org/10.1016/j.ceramint.2012.09.025

sintering bodies from a powder consisting of particles having SiC core and SiO_2 shells (hereafter referred to as SiC/SiO_2), this study demonstrates that SiO_2 can be a suitable additive for SiC and can enhance the mechanical properties of the sintered SiC body. We developed a rotary chemical vapor deposition (RCVD) technique to prepare the powder with the core–shell particle powder by depositing a thin layer of SiO_2 on the SiC cores. Previous studies reported that Ni nanoparticles could be prepared [11] and a layer of SiO_2 [12] could be deposited on cubic BN (cBN) powder by RCVD. The resulting composite powder layer could then be consolidated by SPS. The cBN (core)/SiO_2 (shell) powder could be effectively densified as the SiO_2 additive retarded the phase transformation of cBN into hexagonal BN (hBN). In this study, the SiC/SiO_2 powder particles were synthesized by RCVD, and the SiC/SiO_2 composites were produced by SPS.

2. Experimental

β-SiC powder (purity: 99%; average particle size = 0.28 μm; Ibiden, Japan) particles were coated with a layer of SiO_2 by RCVD using tetraethyl orthosilicate ($(C_2H_5O)_4Si$) as a precursor. Fig. 1 shows a schematic of the RCVD process. To suspend the SiC powder properly in the reactant gas, four blades were attached to the inner wall of the reactor as depicted in the inset of Fig. 1.

The SiC powder was placed in the reactor chamber and heated to 898 K. The reactor chamber was rotated at 45 rpm. The liquid precursor $(C_2H_5O)_4Si$ was heated to 363 K and its vapors were introduced into the reactor chamber at a supply rate R_s of 1.25×10^{-6} kg s^{-1} using Ar as a carrier gas. The flow rate of Ar was 8.33×10^{-7} m^3 s^{-1}. O_2 was separately introduced into the reactor chamber at a flow rate of 3.33×10^{-7} m^3 s^{-1}. The total pressure inside the chamber P_{tot} was maintained at 400 Pa, and the total deposition time was 7.2 ks.

The SiC/SiO_2 composite powder thus formed was consolidated by SPS (SPS-210LX, SPS Syntex, Japan). A sample of uncoated monolithic SiC powder was also sintered for comparison purposes. The powder samples to be sintered were poured into a 10 mm inner diameter graphite die. This graphite die was covered with carbon wool that acted as a thermal insulator. The heating rate was 1.7 K s^{-1}, and the soaking time was 0.6 ks. The sintering temperatures ranged from 1723 to 2223 K. The temperature was measured by an optical pyrometer focused on a hole (diameter = 2 mm and depth = 5 mm) in the graphite die. The loading pressure was 100 MPa.

The densities of the sintered bodies formed from the SiC/SiO_2 composite as well as those from the monolithic SiC were measured using Archimedes' method and distilled water. Their values were converted to relative densities using the theoretical densities of β-SiC (3.21 Mg m^{-3}) [2] and SiO_2 (2.20 Mg m^{-3}) [11]. The crystal structures and phases of the sintered SiC/SiO_2 and SiC bodies were identified by X-ray diffraction (XRD) analyses (GRAD-C, Rigaku) using Cu Kα radiation. Their microstructures were observed by transmission electron microscopy (TEM) (EM-002B, TOPCON) and scanning electron microscopy (SEM) (S-3100H, HITACH). The Vickers hardness H_v and fracture toughness K_{IC} of the sintered SiC/SiO_2 and SiC bodies were determined at room temperature using a Vickers microhardness tester (HM-221, Mitutoyo) using loads P of 1.96 and 9.8 N. The hardness and toughness values were determined at 10 different points. The value of H_v (GPa) was calculated using Eq. (1):

$$H_v = 1.854 \times 10^{-9} \times \frac{p}{d^2} \quad (1)$$

where P (N) is the applied load and d (m) is the average value of the two diagonal lengths of the Vickers indentation. The value of K_{IC} (MPa $m^{1/2}$) was found using Eq. (2) [13,14]:

$$K_{IC} = 0.073 \times 10^{-6} \times \frac{p}{c^{3/2}} \quad (2)$$

where c (m) is the average half length of the cracks formed around the corners of the indentations.

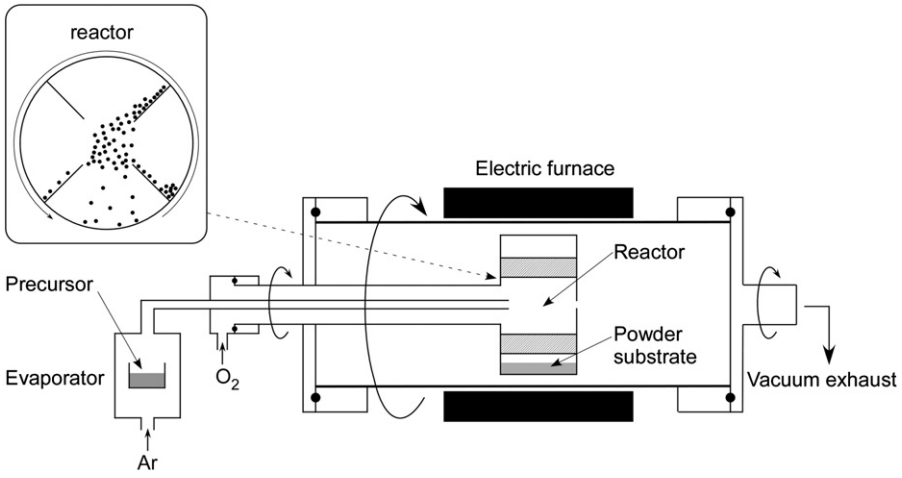

Fig. 1. Schematic of rotary chemical vapor deposition (RCVD) process.

3. Results and discussion

Fig. 2 shows the XRD patterns of the monolithic SiC and SiC/SiO_2 powders. The diffraction peaks at $2\theta = 35.6^\circ$ (111), 41.4° (200), 60.0° (220), 71.8° (311), and 75.5° (222) were assigned to β-SiC (3C). A broad peak at around $2\theta = 22.0^\circ$ was indexed to amorphous SiO_2. No peaks attributable to carbon were found, and the peaks attributable to the β-SiC powder produced no changes in the SiC/SiO_2 powder.

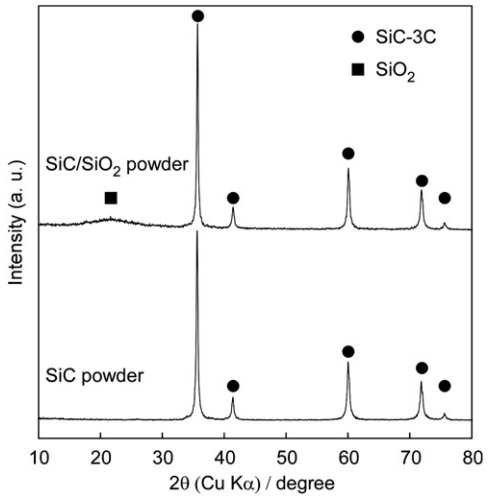

Fig. 2. XRD patterns of SiC/SiO_2 composite and monolithic SiC powders.

Fig. 3(a) shows a TEM image of a particle of the SiC/SiO_2 powder. The layer thickness of the amorphous SiO_2 was 10–15 nm. The SiC/SiO_2 powder weight increased after the RCVD process, and on the basis of this change in weight, the SiO_2 content in the SiC/SiO_2 powder was estimated at 9 mass%. This weight is equivalent to that of an 11 nm thick SiO_2 layer, assuming that the SiC powder particles are uniformly coated by the SiO_2 layer. Thus, the thickness of the SiO_2 layer calculated on the basis of the change in the SiC/SiO_2 powder was almost the same as that determined from the TEM-based observations. Fig. 3(b) shows the diffraction ring for amorphous SiO_2 as well as a set of sharp crystal diffraction spots in the selected area electron diffraction (SAED) pattern for the particles shown in Fig. 3(a). The spots in the SAED pattern were indexed as the (020), (200) and (220) lattice planes of β-SiC (3C).

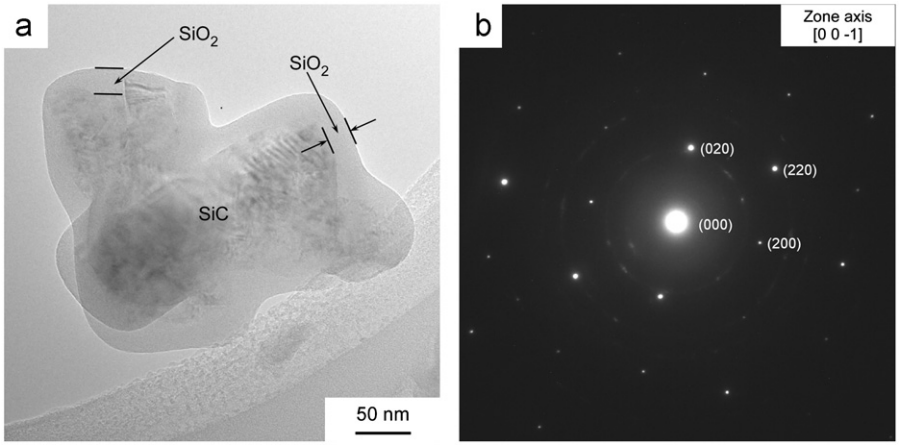

Fig. 3. (a) TEM image of SiC/SiO_2 composite powder particle and (b) SAED pattern of particle shown in (a).

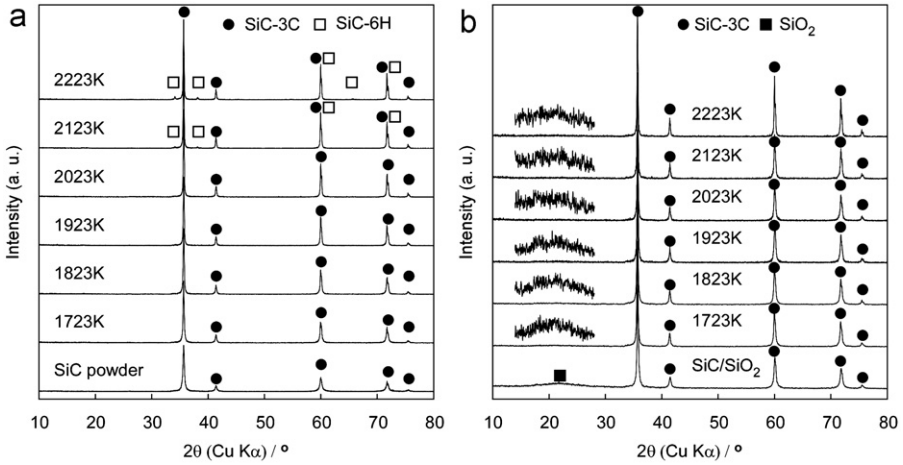

Fig. 4. Effect of sintering temperature on XRD patterns of bodies formed by sintering of (a) monolithic SiC and (b) SiC/SiO_2 composite powder.

Fig. 4(a) and (b) show the XRD patterns of the monolithic SiC and the SiC/SiO_2 bodies sintered at various temperatures, respectively. In the monolithic SiC body, a hexagonal 6H SiC phase was identified at temperatures higher than 2123 K, indicating a phase transformation of 3C into 6H. On the other hand, in the SiC/SiO_2 body, no such phase transformation was observed. The phase transformation of SiC from 3C (a=0.435845 nm, unit cell volume=0.083 nm^3) [15] into 6H (a=0.3081 nm, c=1.51248 nm, unit cell volume=0.144 nm^3) [16] is usually accompanied by volume expansion. However, it is likely that the SiO_2 layer might have prevented a volume increase of the β-SiC particles, thus preventing a phase transformation.

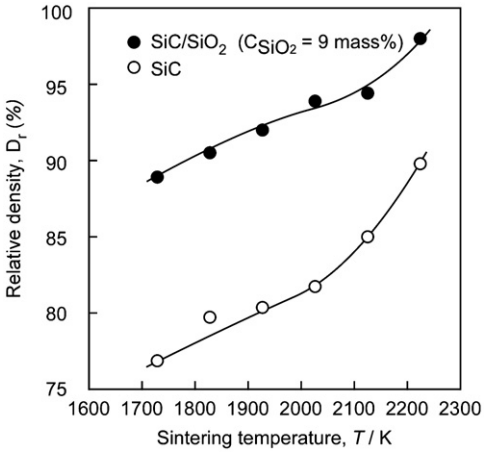

Fig. 5. Relative densities of bodies formed by sintering of monolithic SiC and SiC/SiO_2 composite powder at 1723–2223 K.

Fig. 5 compares the relative densities of the SiC/SiO_2 bodies sintered at 1723–2223 K with those of monolithic SiC bodies. The relative density of the SiC/SiO_2 bodies increased with an increase in the sintering temperature, and the highest value was 98.1% at 2223 K. This was 8–12% higher than the corresponding value of the monolithic SiC body. Fig. 6 shows the SEM images of the monolithic SiC and SiC/SiO_2 sintered bodies. The density and grain size of the sintered monolithic SiC bodies increased with increasing temperature. In addition, the monolithic SiC bodies sintered at 2223 K contained many pores. On the other hand, the density of the sintered

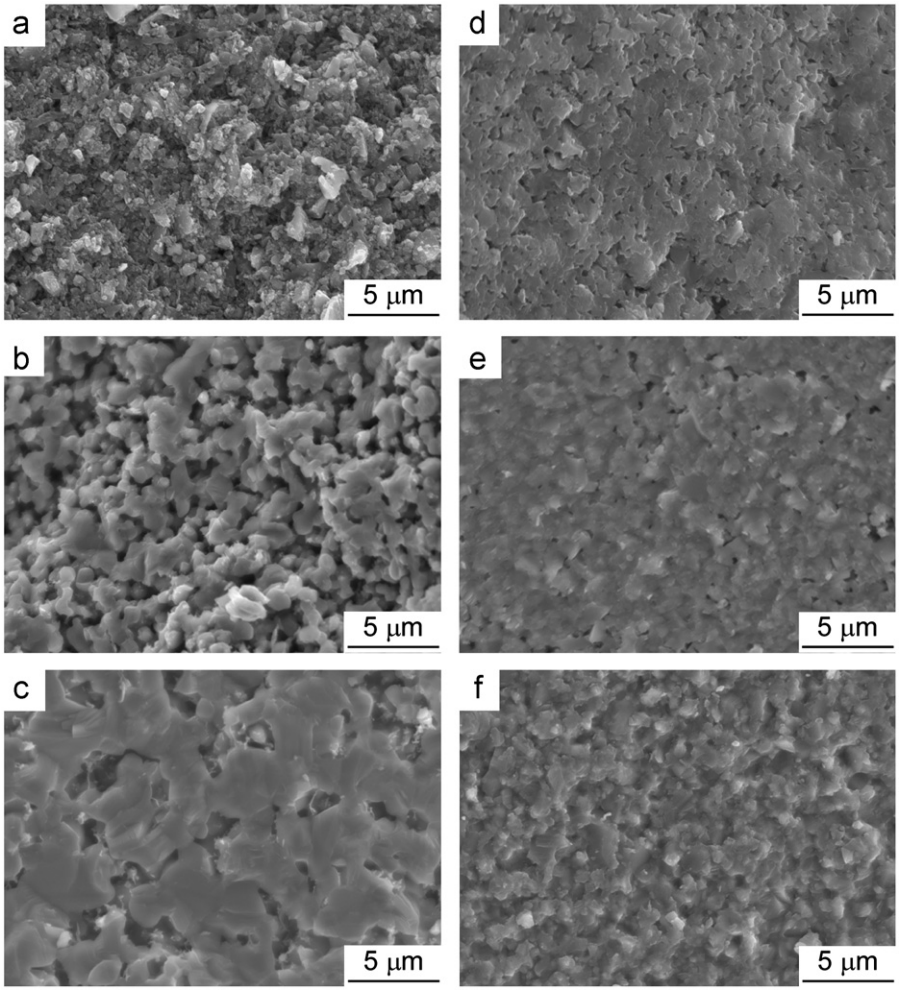

Fig. 6. (a), (b) and (c) Microstructure of a monolithic SiC body and (d), (e) and (f) body formed from SiC/SiO_2 composite powder via SPS at (a) 1723 K, (b) 1923 K, (c) 2223 K, (d) 1723 K, (e) 1923 K and (f) 2223 K.

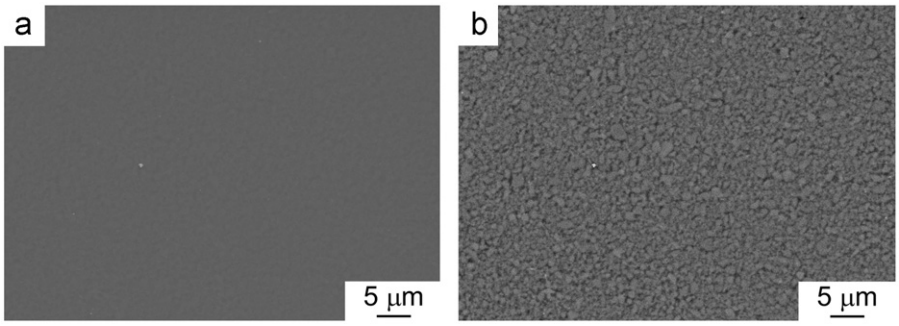

Fig. 7. (a) SEM and (b) back-scattered electron images of body formed by sintering of SiC/SiO_2 composite powder at 2223 K.

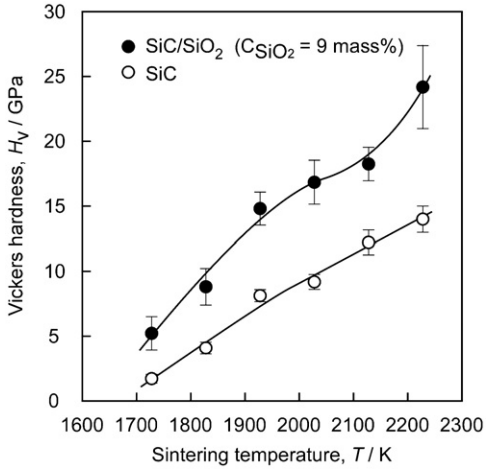

Fig. 8. Effect of sintering temperature on Vickers hardness of bodies formed by sintering of monolithic SiC and SiC/SiO_2 composite powder at 1723–2223 K.

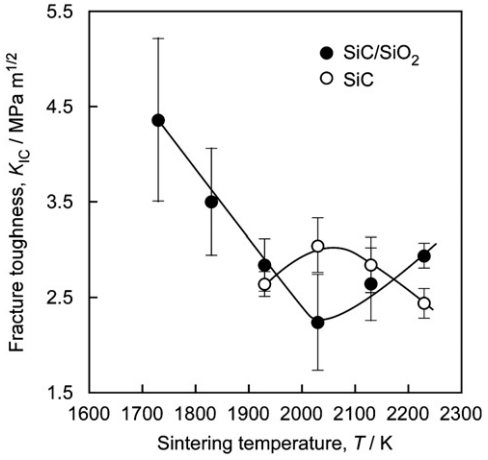

Fig. 9. Effect of sintering temperature on fracture toughness of the bodies formed by sintering of monolithic SiC and SiC/SiO_2 composite powder at 1723–2223 K.

SiC/SiO_2 bodies also increased but their grain size did not. This was due to the SiO_2 layer surrounding the SiC grains. These SiC/SiO_2 bodies had the highest density (98.1%) at 2223 K. The SiO_2 layer around the SiC powder particles significantly promoted the SiC densification and inhibited grain growth.

Fig. 7(a) and (b) show a SEM and a back-scattered electron image of a SiC/SiO_2 body sintered at 2223 K, respectively. Very few pores can be observed in the body. In Fig. 7(b), the black phase is SiO_2 and the grey phase is SiC. SiO_2 is uniformly distributed in the sintered SiC/SiO_2 body, and the SiC phase is separated from the SiO_2 phase. The grains of SiC in the sintered SiC/SiO_2 body were found to be around 500 nm in diameter.

Fig. 8 shows the effects of the sintering temperature on the Vickers hardness H_v of the bodies formed from the sintering of the SiC/SiO_2 composites. The sintering temperature was varied from 1723 to 2223 K. For comparison, the H_v values of the monolithic SiC bodies are also shown. The values of H_v of the sintered SiC/SiO_2 bodies were 5–10 GPa higher than those of the sintered SiC bodies. The SiO_2 layer significantly increased the H_v values of the SiC/SiO_2 bodies. The H_v of the monolithic SiC bodies and that of the SiC/SiO_2 bodies increased continuously with the sintering temperature, and the highest value of H_v for a sintered SiC/SiO_2 body was 24.4 GPa at 2223 K.

Fig. 9 shows the fracture toughness K_{IC} of both the bodies sintered from the SiC/SiO_2 composite powder at 1723–2223 K and those sintered from the monolithic SiC powder. No cracks were observed in the monolithic SiC bodies at 1723 or 1823 K. Of all the SiC/SiO_2 sintered bodies, the one sintered at 1723 K showed the largest K_{IC} (4.4 MPa $m^{1/2}$). This value was more than 1.5 times larger than the highest K_{IC} of the monolithic SiC sintered body at 2023 K. The K_{IC} of the bodies sintered from the SiC/SiO_2 composite powder at temperatures lower than 2023 K decreased with an increase in the sintering temperature. At temperatures higher than 2023 K, the K_{IC} of the SiC/SiO_2 bodies increased slightly with an increase in the sintering temperature. On the other hand, the K_{IC} of the SiC bodies slightly decreased with an increase in the sintering temperature. This difference in the change of K_{IC} was due to the presence of the SiO_2 layer. The SiO_2 layer increased the K_{IC} of the SiC/SiO_2 bodies. In general, a SiC/SiO_2 body sintered at 2223 K had higher H_v and K_{IC} values than those of a monolithic SiC body. This was

probably due to the small grain size of the sintered SiC/SiO_2 bodies, which was around 500 nm.

4. Conclusions

β-SiC powder was uniformly coated with an amorphous SiO_2 layer using the RCVD technique, leading to the formation of a powder with particles that had a SiC core and a SiO_2 shell. The thickness of the amorphous SiO_2 layer was 10–15 nm, and the SiO_2 content in the SiC/SiO_2 composite powder was 9 mass%. The SiC/SiO_2 composite powder was sintered by SPS. The presence of the SiO_2 layer in the bodies formed by the sintering of the SiC/SiO_2 composite powder inhibited the phase transformation of SiC from 3C to 6H. It also inhibited grain growth in SiC. The relative density and Vickers hardness of the sintered SiC/SiO_2 bodies increased with increasing sintering temperature. SiC/SiO_2 composite bodies sintered at 2223 K exhibited the highest density (98.1%) and hardness values (24.4 GPa).

Acknowledgments

This research was supported by the Japan Global COE program; the Institute for Materials Research, Tohoku University; the China Scholarship Council; and the State Key Laboratory of Advanced Technology for Materials Synthesis and Processing, Wuhan University of Technology, PRC.

References

[1] F. Guillard, A. Allemand, J.D. Lulewicz, J. Galy, Densification of SiC by SPS-effects of time, temperature and pressure, Journal of the European Ceramic Society 27 (2007) 2725–2728.
[2] S. Baud, F. Thevenot, Microstructures and mechanical properties of liquid-phase sintered seeded silicon carbide, Materials Chemistry and Physics 67 (2001) 165–174.
[3] R. Riedel, G. Passing, H. Schonfelder, R.J. Brook, Synthesis of dense silicon-based ceramics at low temperatures, Nature 355 (1992) 714–717.
[4] S. Prochazka, Ceramics for high-performance applications, in: Proceedings of the Second Army Materials Technology Conference, Army Materials and Mechanics Research Center (US) Edition, Hyannis, 1974, pp. 239 – 252.
[5] S. Prochazka, et al., Investigation of ceramics for high-temperature turbine vanes, in: Report AD-779 053, General Electric Corporate R&D, New York, 1974.
[6] Z.A. Munir, U. Anselmi-Tamburini, M. Ohyanagi, The effect of electric field and pressure on the synthesis and consolidation of materials: a review of the spark plasma sintering method, Journal of Materials Science 41 (2006) 763–777.
[7] Y. Zhou, K. Hirao, M. Toriyama, H. Tanaka, Very rapid densification of nanometer silicon carbide powder by pulse electric current sintering, Journal of the American Ceramic Society 83 (2000) 654–656.
[8] M. Ohyanagi, et al., Consolidation of nanostructured SiC with disorder–order transformation, Scripta Materialia 50 (2004) 111–114.
[9] H. Ye, G. Rixecker, F. Aldinger, Liquid phase sintered SiC with SiO_2 additive, Ceramics-Processing, Reliability, Tribology and Wear 12 (2006) 173–177.
[10] J.F. Zhang, R. Tu, T. Goto, Fabrication of transparent SiO_2 glass by pressureless sintering and spark plasma sintering, Ceramics International 38 (2012) 2673–2678.
[11] J.F. Zhang, R. Tu, T. Goto, Densification of SiO_2–cBN composites by using Ni nanoparticle and SiO_2 nanolayer coated cBN powder, Ceramics International 38 (2012) 4961–4966.
[12] J.F. Zhang, R. Tu, T. Goto, Preparation of Ni-precipitated hBN powder by rotary chemical vapor deposition and its consolidation by spark plasma sintering, Journal of Alloys and Compounds 502 (2010) 371–375.
[13] A.B.R. Lawn, E.R. Fuller, Equilibrium penny-like cracks in indentation fracture, Journal of Materials Science 10 (1975) 2016–2024.
[14] K. Tanaka, Elastic/plastic indentation hardness and indentation fracture toughness: the inclusion core model, Journal of Materials Science 22 (1987) 1501–1508.
[15] Inorganic Crystal Structure Database (ICSD) No. 28389.
[16] Inorganic Crystal Structure Database (ICSD) No. 156190.